Original Article

Conventional versus cone-beam computed tomography in lung biopsy: diagnostic performance, risks, and the advantages of tract embolization with gelfoam particle suspension

Xugong Zou[1], Ning Cui[2], Qiang Ma[1], Zhipeng Lin[1], Jian Zhang[1], Xiaoqun Li[1]

[1]Department of Interventional Medicine, Zhongshan People's Hospital, Zhongshan, China; [2]Medical Imaging Center, Taihe Hospital, Shiyan, China

Contributions: (I) Conception and design: X Li, X Zou; (II) Administrative support: Z Lin; (III) Provision of study materials or patients: Z Lin, J Zhang; (IV) Collection and assembly of data: Q Ma; (V) Data analysis and interpretation: N Cui, X Zou; (VI) Manuscript writing: All authors; (VII) Final approval of manuscript: All authors.

Correspondence to: Xugong Zou, MD; Xiaoqun Li, MD. Department of Interventional Medicine, Zhongshan People's Hospital, No. 2 Sunwen East Road, Shiqi District, Zhongshan 528403, China. Email: 413607891zxg@163.com; lxq13902827023@163.com.

Background: With the widespread adoption of computed tomography (CT) technology, the number of detected pulmonary nodules has gradually increased. CT-guided percutaneous needle biopsy has become the primary method for qualitative diagnosis of pulmonary nodules. Benefiting from its three-dimensional (3D) reconstruction capability, cone-beam CT (CBCT) technology has also been widely adopted. Nevertheless, pneumothorax remains the most common complication of these diagnostic and therapeutic procedures. This study assessed the diagnostic accuracy of conventional CT (CCT)- and CBCT-guided coaxial core needle biopsy (CCNB) and the effectiveness of gelfoam particle suspension in reducing complications through tract embolization.

Methods: A retrospective analysis was conducted on 320 patients who had undergone CCNB for nodules ≤3 cm from January 2020 to June 2022 at Zhongshan People's Hospital, comprising 325 biopsies (145 CCT-guided and 180 CBCT-guided). Gelfoam tract embolization was specifically used in biopsies of patients identified with a high risk of complications. Comparative statistics involved diagnostic outcomes (sensitivity, specificity, accuracy), procedural lengths, complication occurrences, and radiation doses.

Results: Diagnostically, both CCT (sensitivity 93.3%, specificity 100%, accuracy 94.1%) and CBCT (sensitivity 92.8%, specificity 100%, accuracy 93.8%) offered a similarly high performance. The CCT technique was preferable in terms of shorter median operational times (19 *vs.* 24 minutes; P<0.001) and greater radiation exposure (13.9 *vs.* 10.1 mSv; P<0.001). The complication rates of CBCT and CCT, such as those of pneumothorax (18.9% *vs.* 20.7%; P=0.69) and hemorrhage (23.9% *vs.* 18.6%; P=0.25), were comparable. Of note, the comparison of biopsies with and without gelfoam embolization revealed a marked reduction in postoperative pneumothorax incidence (1.24% *vs.* 7.9%; P=0.004) and the requirement for drainage (0% *vs.* 4.27%; P=0.02), indicating the effectiveness of this procedure.

Conclusions: CCT- and CBCT-guided lung biopsies demonstrate equivalent diagnostic capacities, with CCT providing shorter median operational times. Importantly, gelfoam embolization substantially diminishes the risk of postoperative pneumothorax, underscoring its value in high-risk patients.

Keywords: Cone-beam computed tomography (CBCT); conventional computed tomography (CCT); coaxial core needle biopsy (CCNB); gelfoam; pneumothorax

Submitted Feb 25, 2024. Accepted for publication Jul 25, 2024; Published online: 28 August 2024.
doi: 10.21037/qims-24-342
View this article at: https://dx.doi.org/10.21037/qims-24-342

Introduction

With the popularity of computed tomography (CT) and the increase in public health concerns, a growing number of pulmonary nodules are being detected. When malignant lesions are suspected, a percutaneous transthoracic needle biopsy can be conducted to obtain diseased tissues for exhaustive histopathologic diagnoses and treatment-related molecular biology tests, which accounts for the elevated demand for this procedure (1,2).

CT is currently the most widely used guidance method in clinical practice, as it provides high soft-tissue contrast and spatial resolution. Previous studies have demonstrated that CT-guided needle biopsy of pulmonary nodules is highly safe and diagnostically accurate (3-5). In recent years, a new guidance method, cone-beam CT (CBCT), has emerged to compensate for the inability of conventional CT (CCT) to perform three-dimensional (3D) reconstruction and has the advantage of fast multiplanar reconstruction. It has been revealed that CBCT guidance is superior to CCT guidance in terms of puncture needle navigation, which reduces the radiation exposure and procedure time of patients (6,7). However, advances in computer technology and software algorithms have allowed for a progressive increase in the use of CT with the function of 3D reconstruction, which may supplant CBCT as the superior method for guiding needle biopsy of the lungs.

Pneumothorax remains the most common complication of biopsy, typically ranging from 20.5% to 37.5% (8-13). It can cause shortness of breath, chest pain, and even life-threatening conditions. When the degree of pneumothorax is severe or the patient's tolerance is low, thoracic puncture with catheter placement is a common treatment with an occurrence rate of 2–15% (14). The onset of pneumothorax causes discomfort to patients, while increasing their pain and likelihood of unexpected hospitalization.

Several methods have been studied to reduce the incidence rate of pneumothorax induced by biopsy, including the injection of sealing materials into the biopsy puncture tract, such as thrombin, water, and autologous blood clots (15-22). Gelfoam is a kind of embolic agent that is recommended for needle tract embolization due to its absorbability and expansibility. However, the gelfoam slurry used in previous studies was manually created, and its particle diameter could not be accurately evaluated. It was primarily applied using coaxial needles with diameters of 19–20 G (19,23). Grange *et al.* applied the gelfoam in 16- to 18-G coaxial needles, concluding that it could reduce the risk of pneumothorax (24). However, no studies have yet investigated its use in pulmonary nodules ≤3 cm.

We thus conducted a single-center, retrospective cohort study to compare the accuracy, safety, procedure time, and radiation exposure of CCT-guided and CBCT-guided needle biopsies of pulmonary nodules ≤3 cm. Concurrently, we investigated the role of the gelfoam particle suspension in needle tract embolization complications of 17-G coaxial needle biopsies. We present this article in accordance with the STARD reporting checklist (available at https://qims.amegroups.com/article/view/10.21037/qims-24-342/rc).

Methods

Patient information

Data were collected from all patients who underwent coaxial core needle biopsy (CCNB) at Zhongshan People's Hospital from January 2020 to June 2022. The exclusion criteria for patients were as follows: (I) nodule size >30 mm, (II) no pulmonary ventilatory function test results, and (III) preoperative imaging data from other institutions (*Figure 1*). In this study, the choice between CT or CBCT guidance was based on the availability of equipment as per the schedule. All procedures were performed by interventional radiologists with 20 years of biopsy experience.

Ethical statement

This work was approved by the Ethics Committee of Zhongshan People's Hospital (No. 2023-004) and was conducted in accordance with the Declaration of Helsinki (as revised in 2013). Informed consent was obtained from all patients involved in the study.

Preoperative preparation

Before the procedure, all patients underwent enhanced chest CT, pulmonary function test, and laboratory tests. The team (including physicians from the respiratory, imaging, oncology, and thoracic surgery departments) discussed the necessity of biopsies, defined the target nodule for the biopsy, and performed a risk assessment for surgical safety. Subsequently, patients signed an informed consent form for the procedure. The day before the procedure, the patients were trained to breathe in and hold their breath. On the day of the procedure, the target nodule for the biopsy was reconfirmed, and the puncture path was designed to avoid

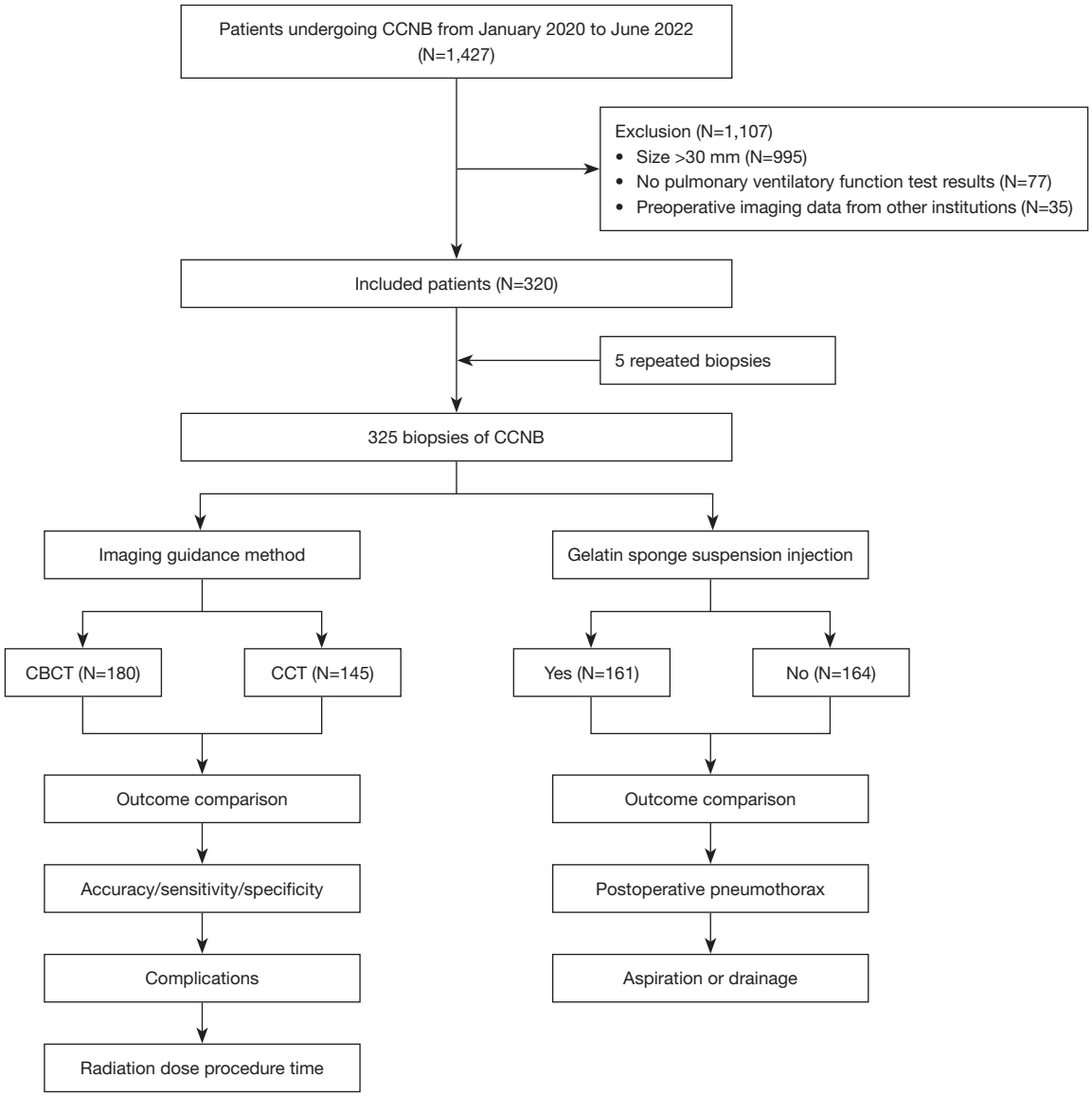

Figure 1 Flow diagram of the study. CCNB, coaxial core needle biopsy; CBCT, cone-beam computed tomography; CCT, conventional computed tomography.

dangerous structures that could cause complications, such as blood vessels, pneumatoceles, and interlobar fissures. Gelatine sponge particles could be injected or to minimize the incidence of complications based on the accumulation of risk factors for complications.

CCT guidance

Guided by a large-aperture CT simulation positioning system (Discovery RT Gen 3, GE HealthCare, Chicago, IL, USA), featuring up to an 80-cm extended display field of view (FOV) and equipped with free-breathing gating technology, a low-dose CT (LDCT) scanning program for lung biopsies was selected, optimizing patient safety and minimizing radiation exposure. A whole-lung scan with a layer thickness of 5 mm was initiated after the breath-holding of patients was detected. The scanning parameters were as follows: voltage, 120 kV; current, 60 mA; and pitch, 0.938. Subsequently, the lesion area was scanned with a layer thickness of 1.25 mm, and 3D images were generated

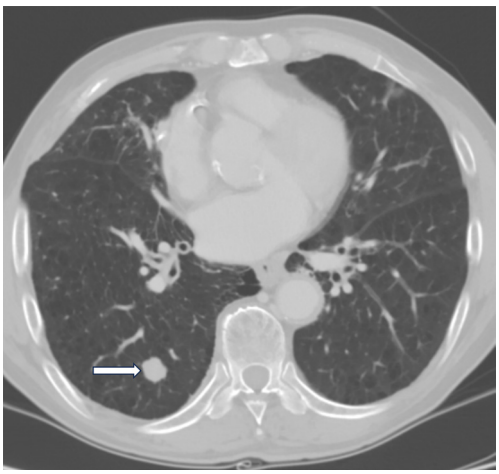

Figure 2 A 71-year-old man with a history of lung cancer after surgery. CT showed a 13 mm × 13 mm nodule (white arrow) in the lower right lung. Pulmonary function tests indicated GOLD 3 (severe). CT, computed tomography; GOLD, Global Initiative for Chronic Obstructive Lung Disease.

using the reform program. Based on the 3D imaging results, a suitable puncture path was selected. Patients were required to hold their breath during the puncture. When the program detected the breath-holding of patients, the interventional radiologist gradually advanced the coaxial needle to the target lung lesion. The interventional radiologist left the operating room and performed the scanning maneuver outside the operating room. Repeated CT scans were performed to ensure that the coaxial needle was correctly positioned, and then a biopsy was completed to obtain the specimen (*Figures 2-4*). Finally, a final CT scan was conducted to assess the complications of the procedure (hemorrhage and pneumothorax).

CBCT guidance

Data were acquired with XperCT software in combination with an Allura Xper FD20 C-arm X-ray system (Philips, Amsterdam, the Netherlands) and sent to the postprocessing

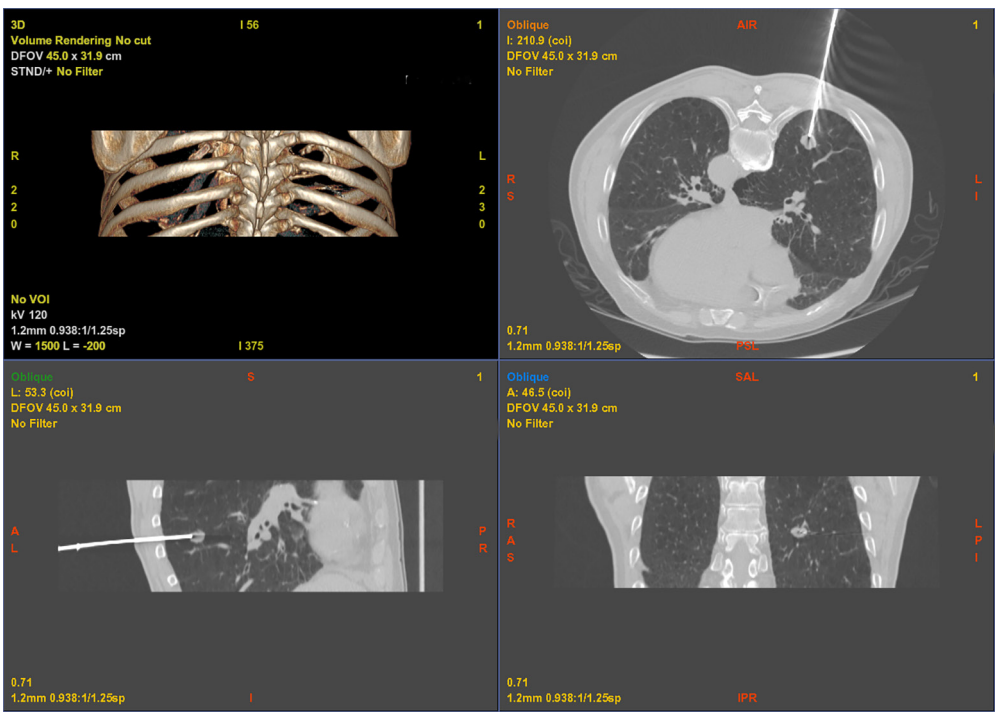

Figure 3 Under the guidance of three-dimensional reconstruction, the coaxial needle completed one puncture to reach the edge of the pulmonary nodule. 3D, three-dimensional; DFOV, display field of view; STND, standard; VOI, volume of interest; R, right; L, left; RS, right superior; LI, left inferior; AIR, anterior inferior right; PSL, patient safety limit; AL, anterior left; PR, posterior right; S, superior; I, inferior; RAS, right anterior superior; LPI, left posterior inferior; SAL, scan axis length; IPR, image processing reconstruction.

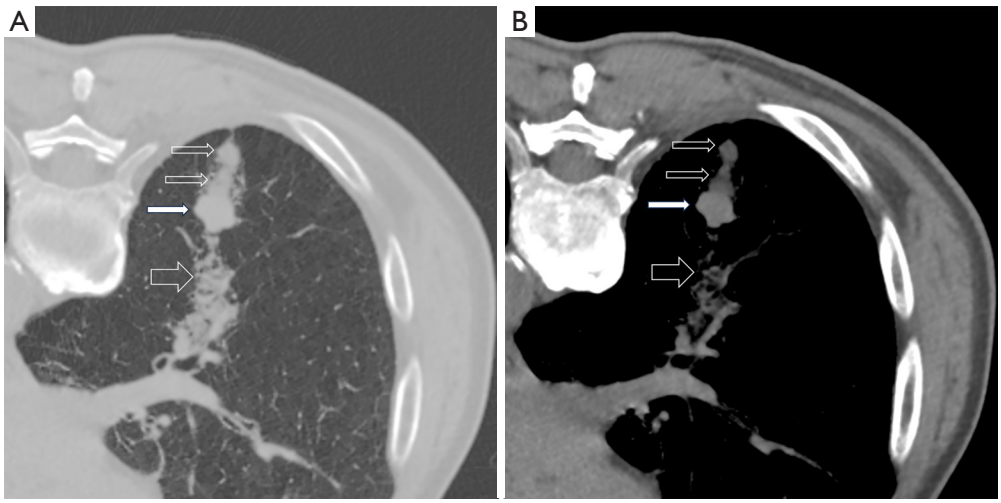

Figure 4 Mild pulmonary hemorrhage was observed on CT. The patient was administered a gelatin sponge particle suspension. (A) The pulmonary window revealed minimal alveolar hemorrhage (wide arrows), with the needle path occluded by a gelatin sponge particle suspension (hollow arrows). (B) The mediastinal window displayed the gelatin sponge particle suspension with a density inferior to that of the pulmonary nodules (white arrows), delineating a clear contrast. CT, computed tomography.

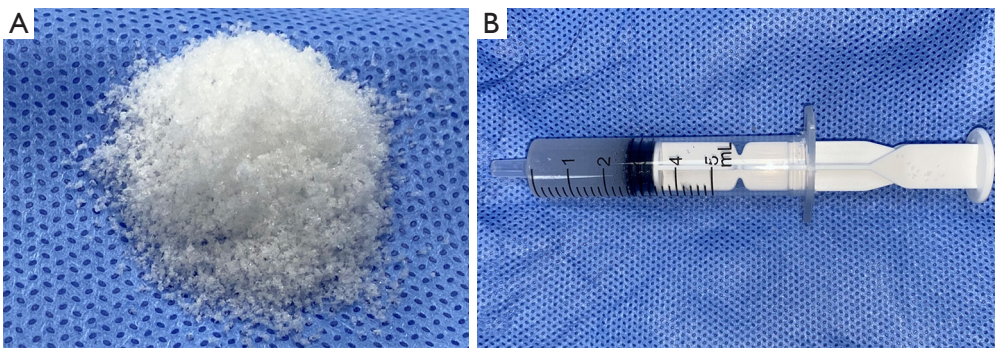

Figure 5 A gelfoam particle suspension was prepared. (A) Premanufactured gelfoam particles, measuring 560–710 μm in diameter and amounting to at least 100 mg, were used. (B) These were combined with saline to create a 2-mL gelfoam particle suspension.

workstation (XperGuide, Philips) for reconstruction to directly generate isotropic 3D volumetric images as thin as 0.4 mm. The puncture path was selected based on the 3D reconstruction results, and patients were required to hold their breath during the puncture. After the interventional radiologist observed that patients had held their breath, the coaxial needle was gradually advanced to the target lung lesion. The remainder of the procedure was the same as that of CT guidance.

Biopsy

When the 17- G coaxial introducer needle (Argon Medical Devices, Athens, TX, USA) reached the desired position, the stylet was withdrawn and the 18-G biopsy needle (BioPince Full Core Biopsy Instrument, Argon Medical Devices) was advanced for pathologic tissue sampling, with a tissue length of 13 or 23 mm. Since our unit was unable to perform an on-site rapid cytopathological examination, the interventional radiologist needed to determine whether sufficient pathological tissues were available. Patients were injected with a suspension prepared with 3 mL of sponge particles with a diameter of 560–710 μm and 2 mL of normal saline (*Figure 5*) if they met at least one of the following criteria: (I) Global Initiative for Chronic Obstructive Lung Disease (GOLD) pulmonary disease

stages 3 and 4 [grading criteria according to the 2021 GOLD: GOLD 3 (severe), forced expiratory volume in 1 s (FEV1)/forced vital capacity (FVC) <70% and FEV1% ≥30% predicted and <50% predicted; GOLD 4 (extremely severe), FEV1/FVC <0% and FEV1% <30% predicted], (II) intraoperative hemorrhage, (III) pneumothorax, and (IV) age over 70 years. The suspension was injected into the needle tract through the coaxial needle, while the coaxial needle was withdrawn until it exited the pleura. Chest X-ray examination was conducted again within 12 hours in order to postoperatively analyze delayed complications.

Data collection

General information was collected for each biopsy. The detailed information of the nodule, such as size, and location was recorded. For each needle biopsy, the surgical data, including all complications (e.g., pneumothorax, intrapulmonary hemorrhage, hemoptysis, especially hemoptysis, and delayed pneumothorax after injection of gelatin sponge particles), procedure time (from the time the patient entered the operating room until he or she left the operating room), radiation dose, and puncture depth (distance from the pleura to the lesion) were collected. The pathological diagnosis was correct if the pathological examination of the biopsied tissue showed a malignant tumor. Meanwhile, the pathological diagnosis was also considered correct if the biopsied tissue was benign as indicated by the pathological examination and if the benign lesion was confirmed by surgery or had disappeared, shrunk, or stabilized for more than 1 year after treatment. According to the detailed method proposed by Priola *et al.* (25), the biopsy results of pulmonary nodules were categorized as true positive, true negative, false positive, or false negative. The effective dose of CCT was calculated with the following formula: dose = dose – length product × κ factor. That of CBCT was calculated based on the following formula: dose = dose – area product × dose conversion factor. The κ factor of conventional chest CT was 0.0146 mSv/mGy*cm (26). The conversion factor was a previously described factor (0.31 mSv/Gy cm^2) for the Allura Xper FD20 system, which was obtained from a published phantom study (27).

Statistical analysis

SPSS 26.0 software (IBM Corp., Armonk, NY, USA) was used for the comparison of data between groups. Continuous data conforming to normal distribution and homogeneity of variance were compared between the two groups with the independent samples *t*-test and expressed as mean ± standard deviation. Data with skewed distribution were compared with the Mann-Whitney test and are summarized as medians and quartiles. Categorical and count data are presented as frequencies (rates) and were analyzed with the Chi-squared test or Fisher exact test. Receiver operating characteristic (ROC) analysis was performed with the "reportROC" package in R version 4.3.0 (The R Foundation of Statistical Computing). A two-sided test was performed, and a difference was considered statistically significant at P<0.05.

Results

A total of 325 biopsies were performed on 320 consecutive patients, among which 5 repeated biopsies, due to the inability to reach a definitive diagnosis, were considered as new cases. These repeated biopsies were performed using a new needle tract each time with a 17-G coaxial introducer needle. The mean size of the target nodules in these biopsies was 22±5.4 mm, with the longest diameter ranging from 6 to 30 mm.

Pulmonary nodule biopsies were completed in all cases, including 180 under CBCT guidance and 145 under CT guidance. General data are detailed in *Table 1*. There were no significant differences between the two guidance groups in terms of gender (P=0.94), age (P=0.62), and nodule characteristics including size (P=0.66), location (P=0.97), and puncture depth (P=0.68). The percentage of malignant lesions was also similar between the CBCT and CCT groups (77.2% *vs.* 82.1%; P=0.38) (*Table 1*).

Diagnostic performance

In the CBCT and CCT groups, the final diagnosis failed for 19 (10.6%) and 10 biopsies (6.9%), respectively due to insufficient abundance of heteromorphic cells in the tissue specimen or loss to follow-up. False-negative diagnoses were confirmed by surgery in 10 (6.2%) and 8 (5.9%) cases of the two groups, respectively. The sensitivity, specificity, accuracy, positive predictive value, and negative predictive value of the CBCT guidance group were 92.8% [95% confidence interval (CI): 88.5–97.1%], 100% (95% CI: 100–100%), 93.8% (95% CI: 89.7–97.9%), 100% (95% CI: 100–100%), and 68.8% (95% CI: 52.7–84.8%), respectively. Additionally, the CCT guidance group had a sensitivity of

Table 1 Basic characteristics

Variable	Total (n=325)	CBCT (n=180)	CCT (n=145)	t/Z/χ^2	P value
Males, n (%)	205 (64.1)	113 (63.8)	92 (64.3)	0.006	0.94[c]
Age (years), mean (range)	64.78±10.89 (30.0–88.0)	65.04±10.54 (37.0–87.0)	64.44±11.35 (30.0–88.0)	0.496	0.62[a]
Lesion size (mm), n (%)				0.197	0.66[c]
≤20	99 (30.5)	53 (29.4)	46 (31.7)		
>20, ≤30	226 (69.5)	127 (70.6)	99 (68.3)		
Depth in the lung (mm), n (%)				0.256	0.68[c]
≤30	141 (43.4)	76 (42.2)	65 (44.8)		
>30	184 (56.6)	104 (57.8)	80 (55.2)		
Location, n (%)				0.001	0.97[c]
Upper and middle lobe	211 (64.9)	117 (65.0)	94 (64.8)		
Lower lobe	114 (35.1)	63 (35.0)	51 (35.2)		
Procedure time (min), n (IQR)	22.0 (19.0, 26.0)	24.0 (21.0, 27.0)	19.0 (16.0, 22.0)	−10.048	<0.001[b]
Effective dose of X-ray (mSv), n (IQR)	10.70 (9.95, 13.80)	10.10 (9.43, 10.40)	13.90 (13.0, 14.70)	15.052	<0.001[b]
Pneumothorax, n (%)	64 (19.7)	34 (18.9)	30 (20.7)	0.165	0.69[c]
Pulmonary hemorrhage, n (%)	70 (21.5)	43 (23.9)	27 (18.6)	1.319	0.25[c]
Malignant lesions, n (%)	258 (79.4)	139 (77.2)	119 (82.1)	0.856	0.38[c]

[a], the independent samples *t*-test; [b], the Mann-Whitney test; [c], the Chi-square test. CBCT, cone-beam computed tomography; CCT, conventional computed tomography; IQR, interquartile range.

93.3% (95% CI: 88.8–97.8%), a specificity of 100% (95% CI: 100–100%), an accuracy of 94.1% (95% CI: 90–98.2%), a positive predictive value of 100% (95% CI: 100–100%), and a negative predictive value of 66.7% (95% CI: 52.7–84.8%) (*Table 2*).

Complications

Between the CBCT and CCT groups, there was a nonsignificant difference in the incidence of pneumothorax (18.9% *vs.* 20.7%; P=0.69) and hemorrhage (23.9% *vs.* 18.6%; P=0.25). After counting, a total of 161 biopsies were injected with gelfoam particle suspension, with their general information being collected (*Table 3*). Within 12 hours postoperation, chest X-ray examination revealed that in the group injected with gelfoam particle suspension, 2 biopsies (1.24%) developed asymptomatic pneumothorax without undergoing aspiration or tube drainage, whereas, in the noninjected group, 13 biopsies (7.9%) experienced pneumothorax, representing a significant difference (P=0.004), as seen in *Table 4*. Among these, 7 biopsies (4.27%) underwent aspiration or catheter drainage, again representing a significant difference (P=0.02). No biopsied patients developed hemoptysis in the gelfoam particle suspension injection group, and 2 patients (1.22%) experienced mild hemoptysis in the noninjection group, but this did not represent a significant difference (P=0.50). Hemoptysis ceased after treatment. Neither ectopic embolism of the circulatory system nor air embolism was observed.

Radiation dose and procedure time

With both the CBCT-guided and CT-guided biopsies, the effective radiation dose was not normally distributed (Shapiro-Wilk test, P<0.001). Therefore, the medians were compared. The median radiation dose for CBCT-guided biopsies was 10.10 mSv, with the first quartile being 9.43 mSv and the third quartile being 10.40 mSv; meanwhile, the median radiation dose for CCT-guided biopsies was 13.9 mSv, with the first quartile being 13 mSv and the third quartile being 14.7 mSv. The median effective radiation dose for CBCT-

Table 2 Histological diagnosis with CBCT-guided and CCT-guided biopsies

Diagnosis	CBCT (n=180)	CCT (n=145)
Malignant lesions, n (%)	139 (77.2)	119 (82.1)
Adenocarcinoma	63	59
Squamous cell carcinoma	23	18
Small cell carcinoma	5	2
Metastases	38	35
Unspecified cancer	7	5
Neuroendocrine tumor	3	–
Benign lesions, n (%)	22 (12.2)	16 (11.0)
Inflammatory infiltrates	11	9
Tuberculosis	7	5
Fungal infection	1	–
Pneumoconiosis	–	1
Epithelioid granulomas	3	1
Indeterminate lesions, n (%)	19 (10.6)	10 (6.9)
Sensitivity, % (95% CI)	92.8 (88.5–97.1)	93.3 (88.8–97.8)
Specificity, % (95% CI)	100.0 (100.0–100.0)	100.0 (100.0–100.0)
Accuracy, % (95% CI)	93.8 (89.7–97.9)	94.1 (90.0–98.2)
PPV, % (95% CI)	100.0 (100.0–100.0)	100.0 (100.0–100.0)
NPV, % (95% CI)	68.8 (52.7–84.8)	66.7 (52.7–84.8)

CBCT, cone-beam computed tomography; CCT, conventional computed tomography; CI, confidence interval; PPV, positive predictive value; NPV, negative predictive value.

guided biopsies was 27.3% lower than that for CCT-guided biopsies (*Figure 6*), which was statistically different (Mann-Whitney test; P<0.001). Significant differences were observed in the median procedure time between patients undergoing CCT-guided and CBCT-guided biopsies (19 *vs.* 24 min; P<0.001). Additionally, the median procedure time between groups with and without gelfoam suspension was assessed (23 *vs.* 21 min; P=0.19), showing no statistically significant difference.

Discussion

Recently, CBCT-guided pulmonary biopsies have attracted widespread attention as an emerging technology. Several studies have demonstrated that CBCT-guided pulmonary biopsies have comparable diagnostic performance and safety to CCT-guided pulmonary biopsies (7,8,28,29). Furthermore, the 3D reconstruction function and open-frame design offer unique advantages to CBCT (30). Specifically, the 3D reconstruction function of CBCT provides accurate positioning and puncture needle navigation. In other words, the target nodule and the puncture path are visualized by CBCT (31), enabling physicians to more accurately guide the needle tip to the target area, which enhances the accuracy and success of the puncture. Additionally, the open-frame design of CBCT provides a larger surgical space, which increases the flexibility and FOV of surgeons as compared to the closed-rack structure of CCT guidance systems. Although the resolution of CBCT is not as high as that of CCT, lung tissues have excellent self-contrast under CBCT, which is sufficient for puncture guidance in intrapulmonary lesions. The 3D reconstruction function of CT is being widely used as computer technology and software algorithms evolve. Fortunately, CT guidance systems are now capable of achieving high-quality 3D image reconstruction and

Table 3 Basic information of patients injected with gelatin sponge suspension

Variable	Total (n=325)	Gelatin sponge suspension injection		t/Z/χ^2	P value
		Yes (n=161)	No (n=164)		
Males, n (%)	205 (64.1)	116 (73.4)	89 (54.9)	11.925	<0.001[c]
Age (years), mean (range)	64.78±10.89 (30.0–88.0)	74.8±3.27 (70.0–88.0)	60.44±5.55 (30.0–69.0)	28.352	<0.001[a]
Lesion size (mm), n (%)				8.308	0.004[c]
≤20	99 (30.5)	61(37.9)	38 (23.2)		
>20, ≤30	226 (69.5)	100 (62.1)	126 (76.8)		
Depth in the lung (mm), n (%)				1.329	0.25[c]
≤30	141 (43.4)	75 (46.6)	66 (40.3.0)		
>30	184 (56.6)	86 (53.4)	98 (59.7.0)		
Location, n (%)				2.302	0.13[c]
Upper and middle lobe	211 (64.9)	98 (60.9)	113 (68.9)		
Lower lobe	114 (35.1)	63 (39.1)	51 (31.1)		
Procedure time (min), n (IQR)	22.0 (19.0, 26.0)	23.0 (18.0, 27.0)	21.0 (17.0, 25.0)	–1.315	0.19[b]
Effective dose of X-ray (mSv), n (IQR)	10.70 (9.95, 13.80)	12.6 (9.76, 14.6)	12.4 (9.45, 14.48)	–1.119	0.26[b]
GOLD, n (%)				–	<0.001[c]
GOLD 1–2	223 (68.6)	59 (36.6)	164 (100)		
GOLD 3–4	102 (31.4)	102 (63.4)	0 (0)		

[a], the independent samples *t*-test; [b], the Mann-Whitney test; [c], the Chi-squared test. GOLD, Global Initiative for Chronic Obstructive Lung Disease; IQR, interquartile range.

Table 4 Complications after injection of gelatin sponge suspension

Variable	Total (n=325)	Gelatin sponge suspension injection		χ^2	P value
		Yes (n=161)	No (n=164)		
Pneumothorax	64 (19.7)	51 (31.7)	13 (7.9)	28.978	<0.001
Intraoperative pneumothorax	49 (15.1)	49 (30.4)	0	–	<0.001
Postoperative pneumothorax	15 (4.6)	2 (1.24)	13 (7.9)	8.246	0.004
Hemorrhage	70 (21.5)	68 (42.2)	2 (1.22)	80.878	<0.001
Intraoperative hemorrhage	68 (20.9)	68 (42.2)	0	–	<0.001
Postoperative hemoptysis	2 (0.6)	0	2 (1.22)	–	0.50
Aspiration or drainage	7 (2.2)	0	7 (4.27)	–	0.02

Data are presented as n (%). The P value was calculated with the Chi-squared test.

have CBCT-like positioning and navigation functions. Accordingly, the advantages of CBCT-guided pulmonary biopsies over CCT-guided pulmonary biopsies have gradually diminished with improvements in CT technology although CBCT-guided pulmonary biopsies have been shown to be significantly superior in previous studies (6,7). In our study, a head-to-head, single-center, retrospective analysis of CBCT-guided and CCT-guided pulmonary biopsies was again performed.

A few single-center studies have directly compared

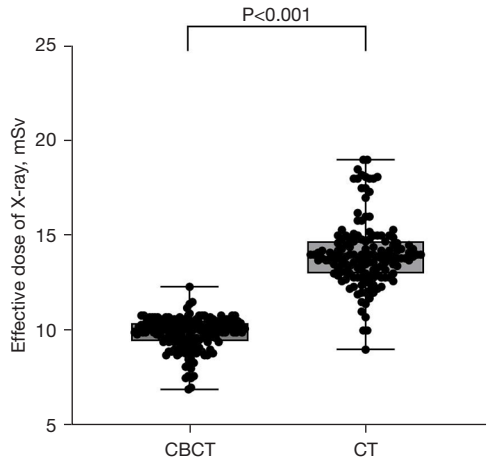

Figure 6 Median effective dose (mSv) for CBCT-guided and CCT-guided biopsies of pulmonary nodules. CBCT, cone-beam computed tomography; CT, computed tomography; CCT, conventional computed tomography.

CBCT-guided and CCT-guided needle biopsies of the lungs (7,8,29,32). In these studies, the sensitivity, specificity, and accuracy were 87–97%, 96.7–100%, and 89–100% for CBCT-guided pulmonary biopsies and 92–100%, 95.7–100%, and 94–100% for CCT-guided pulmonary biopsies, respectively; these findings suggest no statistically significant difference in diagnostic performance between the two imaging-guided modalities, with both modalities demonstrating excellent diagnostic performance. Lee *et al.* (28) performed a multicenter study that included eight medical institutions and 9,239 patients and reported that the sensitivity, specificity, and accuracy of CBCT *vs.* CCT were 95.6% *vs.* 94.8%, 95.5% *vs.* 88.3%, and 95.5 *vs.* 93.3%, respectively. Of note, our study showed similar results, with the sensitivity, specificity, and accuracy of CBCT-guided *vs.* CCT-guided needle biopsies of the lungs being 92.8% *vs.* 93.3%, 100% *vs.* 100%, and 93.8% *vs.* 94.1%, respectively, indicating that both biopsy methods had favorable diagnostic performance.

CBCT not only has the same excellent diagnostic performance as CCT but also facilitates the procedure due its 3D reconstruction function and open-frame design. A meta-analysis revealed a mean total procedure time of 12–32 minutes for CBCT-guided biopsies (33). In previous single-center controlled studies, CBCT-guided biopsies had shorter procedure times than did CCT-guided biopsies (7,32). With the rise in computer processing capabilities and the advancements in iterative reconstruction software algorithms, the duration required by CCT to create 3D images has been markedly reduced, and its image creation speed has now surpassed that of CBCT. This has allowed for the more intuitive planning of puncture paths and reduced the dependence on frame tilting, thus compensating for the inability of CT to rotate the CT gantry. The large-aperture CT simulation positioning device features an 80-cm extended display FOV, providing a larger space for surgical maneuvers, which also diminishes the advantage of CBCT's open-frame design. Moreover, CCT's laser positioning function allows it to complete the first scanning examination faster, and CCT can even more accurately and quickly complete the puncture when combined with respiratory gating. In our study, the procedure time was substantially shorter for CCT-guided pulmonary biopsies than for CBCT-guided pulmonary biopsies (19 *vs.* 24 min; P<0.001). We now prefer to perform lung puncture biopsies under CCT guidance.

Pneumothorax and hemorrhage are the most common complications of pulmonary biopsies, and they have widely varying incidence rates, usually ranging from 20.5% to 37.5% (9-13) and from 10.9% to 21.7% (7,30), respectively, similar to incidence rates in our study. Risk factors for pneumothorax are numerous, including pulmonary emphysema, nodule size, body position, longer puncture distance, multiple puncture, coaxial needle diameter, and subpleural nodules (6,7,10,11,30,34,35). The risk factors of hemorrhage include advanced age and nodule size (30). In general, these complications are detected during the puncture or on immediate review after the tissue specimen has been obtained. Notably, sealing materials such as thrombin, water, and autologous blood clots) have been applied to seal the needle tract (15-22), which has been confirmed to decrease the incidence of pneumothorax and hemorrhage. Gelfoam is recommended for needle tract embolization due to its absorbability and expansibility and has achieved good clinical results. In our study, it was hypothesized that prefabricated gelatin sponge particles are capable of reducing the pneumothorax risk among high-risk patients. The study incorporated samples of nodules smaller than 3 cm in diameter, which are associated with higher puncture difficulties and an increased risk of pneumothorax. The findings underscore the importance of this technique for patients at high risk of pneumothorax, thereby demonstrating its considerable clinical application value. Furthermore, by maintaining the consistency of the sample characteristics, the study minimized the variation in pneumothorax risk caused by differences in nodule

diameter. In contrast, the gelfoam slurry used in previous studies was handmade (19,23,24), making it impossible to accurately assess its particle diameter. During the biopsy or tissue sectioning process, damage to the pulmonary vein can occur (36), and an uncertain particle diameter might increase the risk of ectopic embolization from a pulmonary vein embolus to the circulatory system. Cousin *et al.* reported a case where a 0.8 mm × 3 mm gold marker was implanted via pulmonary puncture for radiotherapy respiratory positioning. A chest CT scan performed immediately after the surgery showed that the gold marker had migrated to the left atrium (37). Olaiya *et al.* reported a case where a 1.2×3 mm gold marker was implanted via pulmonary puncture for localization during pulmonary wedge resection. Intraoperative fluoroscopic evaluation showed that the marker had embolized to the distal left anterior descending artery (38). Therefore, greater attention should be paid to the risk of systemic circulation embolism, especially those particles with uncertain diameters. The smaller the diameter is, the higher the risk, and adopting prefabricated gelfoam particles with precise and consistent sizes is crucial to reducing this risk. After injection of the gelfoam particles, they expand within the needle tract, forming a filling that closely fits the shape of the needle tract. This filling exerts pressure on the surrounding blood vessels and bronchi, effectively preventing bleeding and air from entering the pleural cavity via the puncture channel.

There are few reports on the use of prefabricated gelfoam particles for sealing the puncture path, and there is no consensus on the appropriate choice of particle diameter. Some researchers have reported that using prefabricated gelfoam particles with a diameter of 1,000–1,200 μm to seal the puncture path after lung biopsy can effectively reduce the risk of pneumothorax. We believe that smaller diameters can close smaller blood vessels and bronchi more effectively. A previous study suggested that the diameter of bronchopulmonary anastomoses is about 325 μm (39). Based on this, we use a diameter of 560–710 μm to balance the sealing effect and reduce the risk of systemic circulation embolism. In this study, in patients aged over 70 years with intraoperative pneumothorax or hemorrhage and with GOLD stage 3–4 lung function, needle tract embolization was performed via injection of gelfoam particle suspension. When compared with that of biopsies without injection, the rate of postoperative delayed pneumothorax was significantly lower (1.24% *vs.* 7.9%; P=0.004); the requirement for aspiration or chest drainage was also lower (0% *vs.* 4.27%; P=0.02). Previous studies reported that in patients in whom gelfoam slurry was injected, those needing chest drainage were 3.5–6.9% (19,24). In this study, however, no biopsies required chest drainage after gelfoam particle injection. We consider this to be the result of using gelfoam particle embolization technology for high-risk pneumothorax patients, which prevented the exacerbation of pneumothorax. This in turn reduced the incidence of postoperative delayed pneumothorax and aspiration or tube drainage needs, even when higher-risk 17-G coaxial needle biopsy was used.

We opted for prefabricated gelfoam particles due to their precisely defined particle diameter, reducing the risk of systematic ectopic embolism and increasing the safety of needle tract embolization. Furthermore, this approach can save operation time, especially when pneumothorax is rapidly increasing and needle tract embolization is required. Despite the additional step of applying gelfoam embolization during the procedure, it did not significantly extend the operation time (23 *vs.* 21 min; P=0.19). However, more clinical studies are required on the selection of particle diameter and the preventive strategy of embolization.

In order to compare the effective radiation doses of CCT and CBCT, we need to establish comparable conversion criteria based on prior studies (26,27). Previous single-center comparative studies (8,29,32) reported that the effective radiation dose of CCT was higher than that of CBCT, which is consistent with our results. Meanwhile, another study indicated that CT provided higher-quality images (39). This study examined the application of LDCT in pulmonary CCNB. LDCT is widely used in the diagnosis of lung diseases, especially in lung cancer screening, due to its reduced radiation exposure (40). However, while LDCT reduces the radiation dose, it may impair image clarity and detail, posing challenges for accurate diagnosis and biopsy procedures. Our research specifically focused on the impact of low-dose scanning on the accuracy of lung nodule biopsies. After comprehensively assessing diagnostic performance and complication rates, we found that the radiation dose from LDCT was not only lower—only 27.3% higher than that of CBCT—but also that by optimizing scanning parameters and employing advanced image reconstruction techniques, LDCT could reliably detect nodules smaller than 3 cm without significantly increasing the risk of complications such as pneumothorax or bleeding. This finding has significant implications for balancing image quality with radiation dosage in clinical practice. By exploiting the properties of conventional CT, Kallianos *et al.* developed an LDCT protocol to guide

needle biopsies of the lungs, which can autonomously set the voltage, current, and scanning range while guaranteeing sufficient image quality. The results showed that this protocol reduced the radiation dose by 64.4% (41). Future research needs to focus on optimizing voltage, current, and scanning range to explore the use of LDCT-guided pulmonary biopsy.

Our study has several limitations which should be mentioned. First, we employed a single-center, retrospective design, which might have introduced bias. Second, although we compared two devices, CCT and CBCT, in guiding needle biopsies of the lungs, CBCT is equipped with the latest technology, whereas CCT has more up-to-date software and hardware support. Therefore, the results we observed may not be fully representative of the performance of all CBCT devices. Third, only 1 year of follow-up was completed for biopsies with benign nodules, which might have resulted in bias related to the diagnostic performance.

Conclusions

CCT- and CBCT-guided lung biopsies demonstrate equivalent diagnostic capacities, with CCT providing shorter median operational times. Importantly, gelfoam embolization substantially diminishes the risk of postoperative pneumothorax, underscoring its value in high-risk patients.

Acknowledgments

Funding: None.

Footnote

Reporting Checklist: The authors have completed the STARD reporting checklist. Available at https://qims.amegroups.com/article/view/10.21037/qims-24-342/rc

Conflicts of Interest: All authors have completed the ICMJE uniform disclosure form (available at https://qims.amegroups.com/article/view/10.21037/qims-24-342/coif). The authors have no conflicts of interest to declare.

Ethical Statement: The authors are accountable for all aspects of the work in ensuring that questions related to the accuracy or integrity of any part of the work are appropriately investigated and resolved. This work was approved by the Ethics Committee of Zhongshan People's Hospital (No. 2023-004) and carried out in accordance with the Declaration of Helsinki (as revised in 2013). Informed consent was obtained from all patients involved in the study.

References

1. Gould MK, Donington J, Lynch WR, Mazzone PJ, Midthun DE, Naidich DP, Wiener RS. Evaluation of individuals with pulmonary nodules: when is it lung cancer? Diagnosis and management of lung cancer, 3rd ed: American College of Chest Physicians evidence-based clinical practice guidelines. Chest 2013;143:e93S-e120S.
2. de Margerie-Mellon C, de Bazelaire C, de Kerviler E. Image-guided biopsy in primary lung cancer: Why, when and how. Diagn Interv Imaging 2016;97:965-72.
3. Andrade JR, Rocha RD, Falsarella PM, Rahal Junior A, Santos RSD, Franceschini JP, Fernando HC, Garcia RG. CT-guided percutaneous core needle biopsy of pulmonary nodules smaller than 2 cm: technical aspects and factors influencing accuracy. J Bras Pneumol 2018;44:307-14.
4. Lendeckel D, Kromrey ML, Ittermann T, Schäfer S, Mensel B, Kühn JP. Pulmonary emphysema is a predictor of pneumothorax after CT-guided transthoracic pulmonary biopsies of pulmonary nodules. PLoS One 2017;12:e0178078.
5. Chang YY, Chen CK, Yeh YC, Wu MH. Diagnostic feasibility and safety of CT-guided core biopsy for lung nodules less than or equal to 8 mm: A single-institution experience. Eur Radiol 2018;28:796-806.
6. Yang L, Wang Y, Li L, Liu D, Wu X, Zhang W, Pan F, Liang H, Zheng C. C-Arm Cone-Beam CT Virtual Navigation versus Conventional CT Guidance in the Transthoracic Lung Biopsy: A Case-Control Study. Diagnostics (Basel) 2022;12:115.
7. Rotolo N, Floridi C, Imperatori A, Fontana F, Ierardi AM, Mangini M, Arlant V, De Marchi G, Novario R, Dominioni L, Fugazzola C, Carrafiello G. Comparison of cone-beam CT-guided and CT fluoroscopy-guided

transthoracic needle biopsy of lung nodules. Eur Radiol 2016;26:381-9.
8. Ruud EA, Stavem K, Geitung JT, Borthne A, Søyseth V, Ashraf H. Predictors of pneumothorax and chest drainage after percutaneous CT-guided lung biopsy: A prospective study. Eur Radiol 2021;31:4243-52.
9. DiBardino DM, Yarmus LB, Semaan RW. Transthoracic needle biopsy of the lung. J Thorac Dis 2015;7:S304-16.
10. Fontaine-Delaruelle C, Souquet PJ, Gamondes D, Pradat E, de Leusse A, Ferretti GR, Couraud S. Predictive factors of complications during CT-guided transthoracic biopsy. Rev Pneumol Clin 2017;73:61-7.
11. Mills M, Choi J, El-Haddad G, Sweeney J, Biebel B, Robinson L, Antonia S, Kumar A, Kis B. Retrospective analysis of technical success rate and procedure-related complications of 867 percutaneous CT-guided needle biopsies of lung lesions. Clin Radiol 2017;72:1038-46.
12. Iguchi T, Matsui Y, Tomita K, Uka M, Umakoshi N, Munetomo K, Hiraki T. CT fluoroscopy-guided biopsy of pulmonary lesions contacting the interlobar fissure: An analysis of 72 biopsies. Diagn Interv Imaging 2022;103:302-9.
13. Brioulet J, David A, Sagan C, Cellerin L, Frampas E, Morla O. Percutaneous CT-guided lung biopsy for the diagnosis of persistent pulmonary consolidation. Diagn Interv Imaging 2020;101:727-32.
14. Gupta S, Wallace MJ, Cardella JF, Kundu S, Miller DL, Rose SC; Society of Interventional Radiology Standards of Practice Committee. Quality improvement guidelines for percutaneous needle biopsy. J Vasc Interv Radiol 2010;21:969-75.
15. Baadh AS, Hoffmann JC, Fadl A, Danda D, Bhat VR, Georgiou N, Hon M. Utilization of the track embolization technique to improve the safety of percutaneous lung biopsy and/or fiducial marker placement. Clin Imaging 2016;40:1023-8.
16. Billich C, Muche R, Brenner G, Schmidt SA, Krüger S, Brambs HJ, Pauls S. CT-guided lung biopsy: incidence of pneumothorax after instillation of NaCl into the biopsy track. Eur Radiol 2008;18:1146-52.
17. Li Y, Du Y, Luo TY, Yang HF, Yu JH, Xu XX, Zheng HJ, Li B. Usefulness of normal saline for sealing the needle track after CT-guided lung biopsy. Clin Radiol 2015;70:1192-7.
18. Maybody M, Muallem N, Brown KT, Moskowitz CS, Hsu M, Zenobi CL, et al. Autologous Blood Patch Injection versus Hydrogel Plug in CT-guided Lung Biopsy: A Prospective Randomized Trial. Radiology 2019;290:547-54.
19. Tran AA, Brown SB, Rosenberg J, Hovsepian DM. Tract embolization with gelatin sponge slurry for prevention of pneumothorax after percutaneous computed tomography-guided lung biopsy. Cardiovasc Intervent Radiol 2014;37:1546-53.
20. Zaetta JM, Licht MO, Fisher JS, Avelar RL; Bio-Seal Study Group. A lung biopsy tract plug for reduction of postbiopsy pneumothorax and other complications: results of a prospective, multicenter, randomized, controlled clinical study. J Vasc Interv Radiol 2010;21:1235-43.e1-3.
21. Lang EK, Ghavami R, Schreiner VC, Archibald S, Ramirez J. Autologous blood clot seal to prevent pneumothorax at CT-guided lung biopsy. Radiology 2000;216:93-6.
22. Ahrar JU, Gupta S, Ensor JE, Mahvash A, Sabir SH, Steele JR, McRae SE, Avritscher R, Huang SY, Odisio BC, Murthy R, Ahrar K, Wallace MJ, Tam AL. Efficacy of a Self-expanding Tract Sealant Device in the Reduction of Pneumothorax and Chest Tube Placement Rates After Percutaneous Lung Biopsy: A Matched Controlled Study Using Propensity Score Analysis. Cardiovasc Intervent Radiol 2017;40:270-6.
23. Renier H, Gérard L, Lamborelle P, Cousin F. Efficacy of the tract embolization technique with gelatin sponge slurry to reduce pneumothorax and chest tube placement after percutaneous CT-guided lung biopsy. Cardiovasc Intervent Radiol 2020;43:597-603.
24. Grange R, Sarkissian R, Bayle-Bleuez S, Tissot C, Tiffet O, Barral FG, Flaus A, Grange S. Preventive tract embolization with gelatin sponge slurry is safe and considerably reduces pneumothorax after CT-guided lung biopsy with use of large 16-18 coaxial needles. Br J Radiol 2022;95:20210869.
25. Priola AM, Priola SM, Cataldi A, Errico L, Di Franco M, Campisi P, Molinaro L, Marci V, Novello S, Fava C. Accuracy of CT-guided transthoracic needle biopsy of lung lesions: factors affecting diagnostic yield. Radiol Med 2007;112:1142-59.
26. Deak PD, Smal Y, Kalender WA. Multisection CT protocols: sex- and age-specific conversion factors used to determine effective dose from dose-length product. Radiology 2010;257:158-66.
27. Strocchi S, Colli V, Conte L. Multidetector CT fluoroscopy and cone-beam CT-guided percutaneous transthoracic biopsy: comparison based on patient doses. Radiat Prot Dosimetry 2012;151:162-5.
28. Lee KH, Lim KY, Suh YJ, Hur J, Han DH, Kang MJ, Choo JY, Kim C, Kim JI, Yoon SH, Lee W, Park CM.

Diagnostic Accuracy of Percutaneous Transthoracic Needle Lung Biopsies: A Multicenter Study. Korean J Radiol 2019;20:1300-10.
29. Ren Q, Zhou Y, Yan M, Zheng C, Zhou G, Xia X. Imaging-guided percutaneous transthoracic needle biopsy of nodules in the lung base: fluoroscopy CT versus cone-beam CT. Clin Radiol 2022;77:e394-9.
30. Fior D, Vacirca F, Leni D, Pagni F, Ippolito D, Riva L, Sironi S, Corso R. Virtual Guidance of Percutaneous Transthoracic Needle Biopsy with C-Arm Cone-Beam CT: Diagnostic Accuracy, Risk Factors and Effective Radiation Dose. Cardiovasc Intervent Radiol 2019;42:712-9.
31. Jiao D, Yuan H, Zhang Q, Han X. Flat detector C-arm CT-guided transthoracic needle biopsy of small (≤2.0 cm) pulmonary nodules: diagnostic accuracy and complication in 100 patients. Radiol Med 2016;121:268-78.
32. Cheng YC, Tsai SH, Cheng Y, Chen JH, Chai JW, Chen CC. Percutaneous Transthoracic Lung Biopsy: Comparison Between C-Arm Cone-Beam CT and Conventional CT Guidance. Transl Oncol 2015;8:258-64.
33. Yan GW, Bhetuwal A, Yan GW, Sun QQ, Niu XK, Zhou Y, Li LF, Li BZ, Zeng H, Zhang C, Li B, Xu XX, Yang HF, Du Y. A Systematic Review and Meta-Analysis of C-Arm Cone-Beam CT-Guided Percutaneous Transthoracic Needle Biopsy of Lung Nodules. Pol J Radiol 2017;82:152-60.
34. Zhou M, Wang T, Wei D, Zhu Y, Jiang Y, Zuo C, Jiang L, Chen H, Guo S, Yang L. Incidence, severity and tolerability of pneumothorax following low-dose CT-guided lung biopsy in different severities of COPD. Clin Respir J 2021;15:84-90.
35. Zhao Y, Wang X, Wang Y, Zhu Z. Logistic regression analysis and a risk prediction model of pneumothorax after CT-guided needle biopsy. J Thorac Dis 2017;9:4750-7.
36. Zhang H, Wang S, Zhong F, Liao M. Risk factors for air embolism following computed tomography-guided percutaneous transthoracic needle biopsy: a systematic review and meta-analysis. Diagn Interv Radiol 2023;29:478-91.
37. Cousin F, Gérard L, Joskin J. Left Cardiac Migration of a Lung Fiducial Marker. J Vasc Interv Radiol 2019;30:445.
38. Olaiya B, Gilliland CA, Force SD, Fernandez FG, Sancheti MS, Small WC. Preoperative Computed Tomography-Guided Pulmonary Lesion Marking in Preparation for Fluoroscopic Wedge Resection-Rates of Success, Complications, and Pathology Outcomes. Curr Probl Diagn Radiol 2019;48:27-31.
39. Yoon W, Kim JK, Kim YH, Chung TW, Kang HK. Bronchial and nonbronchial systemic artery embolization for life-threatening hemoptysis: a comprehensive review. Radiographics 2002;22:1395-409.
40. Jin S, Zhang B, Zhang L, Li S, Li S, Li P. Lung nodules assessment in ultra-low-dose CT with iterative reconstruction compared to conventional dose CT. Quant Imaging Med Surg 2018;8:480-90.
41. Kallianos KG, Elicker BM, Henry TS, Ordovas KG, Nguyen J, Naeger DM. Instituting a Low-dose CT-guided Lung Biopsy Protocol. Acad Radiol 2016;23:1130-6.

Cite this article as: Zou X, Cui N, Ma Q, Lin Z, Zhang J, Li X. Conventional versus cone-beam computed tomography in lung biopsy: diagnostic performance, risks, and the advantages of tract embolization with gelfoam particle suspension. Quant Imaging Med Surg 2024;14(9):6479-6492. doi: 10.21037/qims-24-342

